Polymer-Nanocarbon Topological and Electronic Interface

Nirmalraj, Peter; dos Santos, Maria Cristina; Rios, Jorge Mario Salazar; Davila, Diana; Vargas, Fiorella; Scherf, Ullrich; Loi, Maria Antonietta

Published in:
Langmuir

DOI:
10.1021/acs.langmuir.8b00485

Publication date:
2018

LANGMUIR Article
Cite This: Langmuir 2018, 34, 6225−6230
pubs.acs.org/Langmuir

Polymer−Nanocarbon Topological and Electronic Interface

Peter Nirmalraj,*[,†,‡] Maria Cristina dos Santos,[§] Jorge Mario Salazar Rios,[§] Diana Davila,[†] Fiorella Vargas,[†,⊥] Ullrich Scherf,[∥] and Maria Antonietta Loi[§]

[†]IBM Research − Zurich, Säumerstrasse 4, CH-8803 Rüschlikon, Switzerland
[‡]Adolphe Merkle Institute, University of Fribourg, Chemin des Verdiers 4, CH-1700 Fribourg, Switzerland
[§]Photophysics and OptoElectronics, Zernike Institute of Advanced Materials, University of Groningen, Groningen 9747, The Netherlands
[∥]Macromolecular Chemistry, Bergische Universität Wuppertal, Gauss-Str. 20, D-42119 Wuppertal, Germany

Supporting Information

ABSTRACT: The electronic structure of semiconducting carbon nanotubes selected through polymer functionalization is routinely verified by measuring the spectral van Hove singularity signature under ultraclean vacuum conditions. Interpreting the effect of unperturbed polymer adsorption on the nanotube energetic bands in solvent media is experimentally challenging owing to solvent molecular crowding around the hybrid complex. Here, a liquid-based scanning tunneling microscope and spectroscope operating in a noise-free laboratory is used to resolve the polymer-semiconducting carbon-nanotube-underlying graphene heterostructure in the presence of encompassing solvent molecules. The spectroscopic measurements highlight the role of polymer packing and graphene landscape on the electronic shifts induced in the nanotube energy bands. Together with molecular dynamics simulations, our experimental findings emphasize the necessity of recording physicochemical and electronic properties of liquid-phase solubilized hybrid materials in their native state.

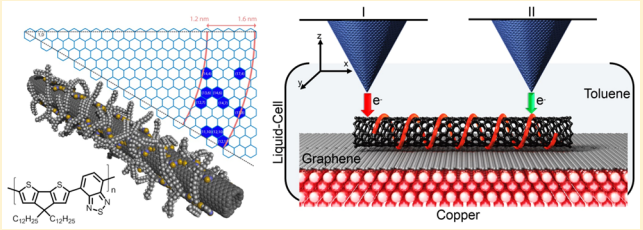

INTRODUCTION

Device scaling requires dimensional shrinking of interconnects. Semiconducting single-walled carbon nanotubes (SWCNT) are one such nanometer-sized electronic material of interest as active electronic component in circuits.[1−3] The challenge is to deliver purely semiconducting SWCNTs in a low-cost and scale-invariant process compatible with a sub-10 nm manufacturing process.[3] Wrapping carbon nanotubes with polymeric molecules[4−10] is a well-established method to segregate semiconducting tubes from their metallic counterparts in thermodynamically stable solutions. The onus then is to select polymeric materials that can both serve as good SWCNT dispersants and possess the right band gap in order to improve the electronic properties of the hybrid material.[5] Prior to integrating these functional hybrid materials in transistors operating at kilohertz range switching speeds with high on/off ratios[11] and in emerging disciplines such ranging from plant nanobionics[12,13] to neuromorphic computing,[14,15] a detailed understanding of their electronic structure, conduction modes of these liquid-solublized materials as it interfaces with solvent molecules is required. The general structure of the polymer−carbon nanotube complex has been studied through atomic force microscopy[11,16,17] under ambient conditions and with high-resolution scanning tunneling microscopy[18] and spectroscopy techniques,[19] where the polymer wrapping angle and energy gaps are resolved under ultrahigh vacuum conditions. Optical spectroscopy techniques[8,16,20,21] have also been successful in decoding the interactions between the non-covalently wrapped polymer and carbon nanostructures but in liquid phase where the structural integrity of the polymer−nanotube complex is not compromised.

In general, it would be highly desirable to extract information on the factors controlling electronic transport through polymer wrapped single walled carbon nanotube (PW-SWCNT) under ambient conditions that is relevant to device fabrication and operation. Successful experiments in this direction will bridge the gap between engineering novel polymer functionalized semiconducting nanotubes and emerging device architectures. However, the challenge is to devise experiments that can verify the structure−function relationship of the polymer−nanotube complex at the atomic scale without denaturing the polymer structure hence requiring measurements directly on the hybrid complex in the presence of solvents used to solubilize the PW-SWCNTs. We resolve with high spatial and energy resolution the electronic structure of the PW-SWCNTs buried in solvent molecules at room-temperature. Our findings indicate the polymer assembly modes to have a direct impact on the density of the states of the semiconducting nanotube verified through liquid-based scanning tunneling microscopy (STM) and spectroscopy (STS). We observe the polymeric strands to

Received: February 12, 2018
Revised: April 6, 2018
Published: May 7, 2018

DOI: 10.1021/acs.langmuir.8b00485
Langmuir 2018, 34, 6225−6230

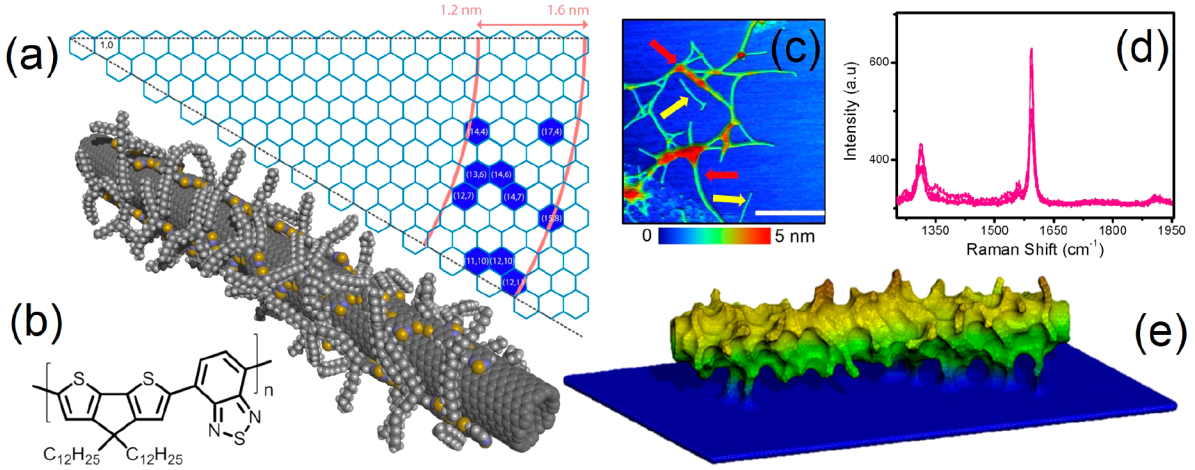

Figure 1. (a) Chirality map and MD simulation snapshot of polymer-wrapped single-walled carbon-nanotube structure. (b) Chemical structure of P12CPDTBT polymeric molecule. (c) Topography of sparsely connected PW-SWCNT network deposited on SiO_2 surface acquired through atomic force microscopy operated in intermittent-contact mode (scale bar: 50 nm). (d) Raman spectrum acquired over a sparse PW-SWCNT network (excitation 473 nm). (e) Molecular surface from a molecular dynamics snapshot of the nanotube−polymer−solvent−graphene system.

spatially distance the nanotube and the metal substrate, resulting in reduced metal induced hybridization of carbon nanotube energy levels for nanotubes with closely packed polymeric molecules. Combined with atomic-scale molecular dynamics (MD) simulations we elucidate the elemental structural and electronic polymer−nanotube interface in a solvent environment at room-temperature.

RESULTS AND DISCUSSION

In this work, we focus on poly[2,6-(4,4-bis(2-dodecyl)-4*H*-cyclopenta[2,1-*b*;3,4*b*′]dithiophene)-*alt*-4,7(2,1,3-benzothiadiazole)] (P12CPDTBT) conjugated polymeric molecules wrapped around semiconducting-SWCNTs synthesized via the arc discharge technique (SO) and dispersed in toluene (see Supporting Information S1 for details on PW-SWCNT solution synthesis). Figure 1a is a detailed chirality map together with a MD simulation snapshot of P12CPDTBT wrapped SWCNT structure. The chemical structure of the polymeric molecule is shown in Figure 1b. For this study, we have selected the SO tubes with larger diameter and catalyst particle-free as the backbone over which the polymers assemble. The PW-SWCNT solution is deposited (2 μL of 10^{-3} M concentration) onto chemical vapor deposition-grown graphene on Cu foil for STM/STS analytics, respectively. In order to study the topology and chemical structure of the hybrid complex, PW-SWCNTs in liquid-phase were deposited onto SiO_2 surface and studied via colocalized AFM and Raman spectroscope (see S2 section in Supporting Information for details on the experimental setup). Figure 1c is a tapping-mode AFM topographic image of a sparsely connected PW-SWCNT networks composed of individual tubes (indicated by yellow arrow) and bundles (indicated by red arrow). Following our section analysis of ∼30 individual tubes registered by tapping-mode AFM, we calculated the mean diameter and length to be (1.3 ± 0.2) nm and (0.8 ± 0.5) μm. Closer examination of the AFM image reveals local height variations, shown by the color code along the nanotube sidewalls and a more prominent increase in height profiles at the junction sites between adjoining tubes. However, neither the polymer structure nor the wrapping angle of the polymer backbone is resolved from such AFM topographic profiles acquired under ambient conditions. The corresponding Raman spectrum (Figure 1d) acquired over the nanotubes within the specific frame as shown in Figure 1c exhibits sharp peaks centered around 1300 and 1600 cm^{-1} which can be associated with the G bands for metallic and semiconducting SWCNTs. The ratio between the two bands and the symmetric shape of the peaks shows that the sample is mostly composed by semiconducting species.[22] The band located between 1300 and 1350 cm^{-1}, could be attributed to the D band which is activated in all forms of carbon consisting of sp2 sites stemming from defects lowering the crystal symmetry.[23] Conversely, previous Raman studies on PCPDTBT polymeric molecules[24] report on sharp peaks centered around 1350 cm^{-1} indicating that the peak we observe near 1340 cm^{-1} stems from the defects on the carbon backbone induced by sonication and from the conjugated polymer.

To clarify the wrapping mechanism of P12CPDTBT around SWCNTs at experimentally inaccessible time scales we rely on atomistic simulations. The nanotube (12,10) was chosen for the MD simulations because it is one of the selected nanotubes by P12CPDTBT polymers with a diameter of ∼1.5 nm, which is representative of the SWCNT source used in the experimental part of this work. The simulations were carried out in two steps: first, the nanotube-polymer-toluene system was equilibrated after a 920 ps MD run. Then a graphene sheet was added and the system was allowed to equilibrate for more than 830 ps. The structure obtained upon classical MD simulation is shown in Figure 1e, where the alkyl tails interface periodically with the graphene surface according to the polymer helical pitch. In particular, the polymeric strands appear to wrap a single nanotube side-by-side in a single helix where one of the alkyl tails interdigitates per tail per repeat unit and the other unit points outward thereby stabilizing the hybrid complex. To quantify the polymer−nanotube binding energy we perform third-order self-consistent charge density-functional tight-binding with empirical dispersion (DFTB3-D3) calculations. We calculate a polymer-carbon nanotube binding energy of 1.31 eV for tubes with indices of (12,10) (see Supporting Information section S3 for MD simulation and binding energy calculation details).

DOI: 10.1021/acs.langmuir.8b00485
Langmuir 2018, 34, 6225−6230

To experimentally verify the assembly and electronic interaction between the polymeric strands on the SWCNTs we conducted high-resolution STM and STS measurements (see schematic representation of the experimental setup in Figure 2a) along the length of the hybrid complex. Previously,

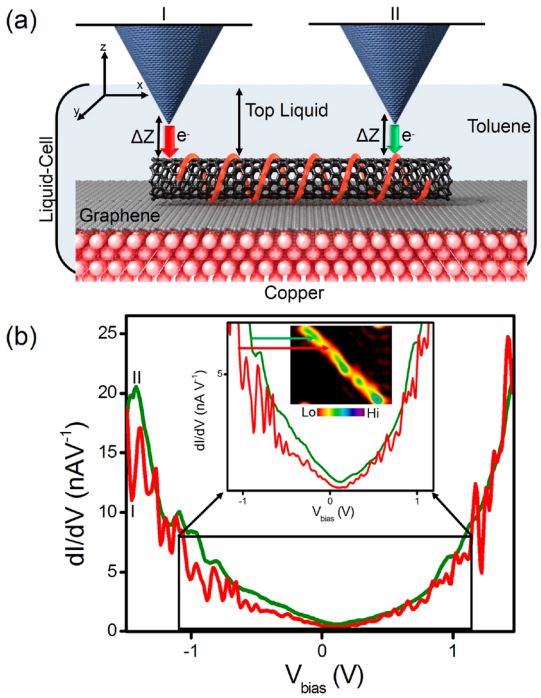

Figure 2. (a) Schematic of a liquid-based scanning tunneling microscope and spectroscope. CVD-grown monolayer graphene on Cu foil is used as the substrate over which PW-SWCNT dispersed in toluene solvent is deposited. The entire sample is placed inside a compact Teflon-based liquid cell. (b) Point-probe spectroscopic analysis of local density of states measured over nonfunctionalized SWCNT (red spectra) and over polymer-wrapped area on SWCNT sidewall (green spectra) (set point parameters: I_t = 180 pA, V_b = 0.5 V). The PW-SWCNT over which the dI/dV spectroscopic curves were acquired is also represented in a constant-current STM image in the inset in panel b. (Scan parameters: tunnel current set point (I_t) = 8 pA, sample bias (V_b) = −0.5 V, scan rate = 24 Hz, image size = 3.8 nm × 4.4 nm.)

we have employed this tool for atomic-scale registry of surface-confined soft nanomaterials in a liquid environment.[25−28] Typically, before commencing imaging and spectroscopic analysis of single PW-SWCNTs, the STM tip quality is verified by means of controls where the atomic lattice and bandstructure of the underlying graphene surface is resolved (see Figure S1, Supporting Information) in toluene environment. A spatially magnified constant-current STM image of a single PW-SWCNT (tube diameter: ∼1.5 nm) is shown in the inset of Figure 2b. The well-defined carbon nanostructure, coiled polymer layer and a clean underlying graphene surface as seen from the STM image are shielded from ambient contamination by the toluene layer, thereby allowing reliable reproduction of the surface topology with spatial information content on par with STM studies under UHV conditions.[19,29] It can be seen from the STM image that the polymeric strands do not wrap the tube axis homogeneously over the entire tube length resulting in the presence of small regions with nonfunctionalized nanotube sidewall. The real-space data indicates the possibility of multiple parallel wrapped polymeric arrangement on the nanotube sidewalls and the presence of lateral polymer chains (highlighted by MD simulations, Figure 1e), which was initially suggested by Smalley and co-workers[30] based on MD calculations as a possible energetic configuration.

Upon resolving the polymeric molecules wrapping the nanotube sidewalls with STM we then focus on mapping the intrinsic electronic structure and local density of states (LDOS) of a single PW-SWCNT. Previously the electronic structure of nonfunctionalized nanotubes[31,32] and nanotubes wrapped with polymeric molecules[18,19] were studied in great detail with point-probe STS. Until now, the van Hove singularities associated with the bandstructure,[31] many-body interactions in electronic band gaps of semiconducting nanotubes[33] and charge transmission details from the polymer to the core nanotube[18,19] have been determined unambiguously at room-temperature and on thermally stable platforms (2−10 K) but only under ultraclean UHV settings. Figure 2b is a differential conductance (dI/dV) spectrum, which is a measure of LDOS around the Fermi edge as a function of applied sample voltage acquired over a PW-SWCNT in the presence of toluene under standard laboratory conditions. The STM probe is positioned and dI/dV curves collected over the areas where there are no polymeric strands wrapping the tubes (red spectra, Figure 2b, averaged over 10 individually acquired spectral curves with an acquisition time of ∼3 s per spectrum) and over regions where the polymeric molecules are clearly discernible from the STM topographic profile. The feedback loop is reinitiated between successive spectral data-acquisition steps, and the nanotube segment is imaged to ensure the exact probe position. The spectral data acquired over the nonfunctionalized region of the nanotube is dominated by sharp energetic peaks (red spectra Figure 2b) observed closer to the Fermi edge. It is known that P12CPDTBT molecules have a highest occupied molecular orbital (HOMO) and lowest unoccupied molecular orbital (LUMO) gap of ∼1.8 eV[34] and toluene has a HOMO−LUMO gap ∼6.5 eV.[35] Hence the energetic peaks observed closer to the Fermi edge cannot be directly due to solvent medium but the contribution of the polymer electronic states to the nanotube density of states below zero is not negligible (see also the theoretical densities of states in Supporting Information Figure S2). We then measure the energy gap (ΔE) of this nanotube (STM image inset Figure 2b) to be ∼0.5 eV, based on the energy difference between the first van Hove singularities, comparable with previous STS reports on semiconducting nanotubes at 4 K[32] and at room-temperature.[29]

Repositioning, the STM probe onto a polymer-adsorbed area along the carbon nanotube as shown in the STM image inset in Figure 2b and recording dI/dV curves, we observe a contrast in the intensity and number of resolvable energetic peaks (vertically offset green spectra Figure 2b) compared with the dI/dV spectra acquired over the bare nanotube (red spectra Figure 2b). Although the line shapes of the two spectral curves are similar (peaks centered around −0.8 eV), there is an overall reduction in peak intensity as a result of the spectral dampening effect of the polymer on the one-dimensional energy bands associated with the inner carbon nanotube. However, new features appear in the PW-SWCNT spectra, which could evoke the formation of hybrid electronic states, shown recently, for peapod-like hybrids through experimental and density functional theory calculations.[36,37]

In addition to imaging tightly packed polymer strand assembly on the nanotube sidewalls as shown in inset Figure 2b, we also detected spatially well-distanced polymeric

DOI: 10.1021/acs.langmuir.8b00485
Langmuir 2018, 34, 6225−6230

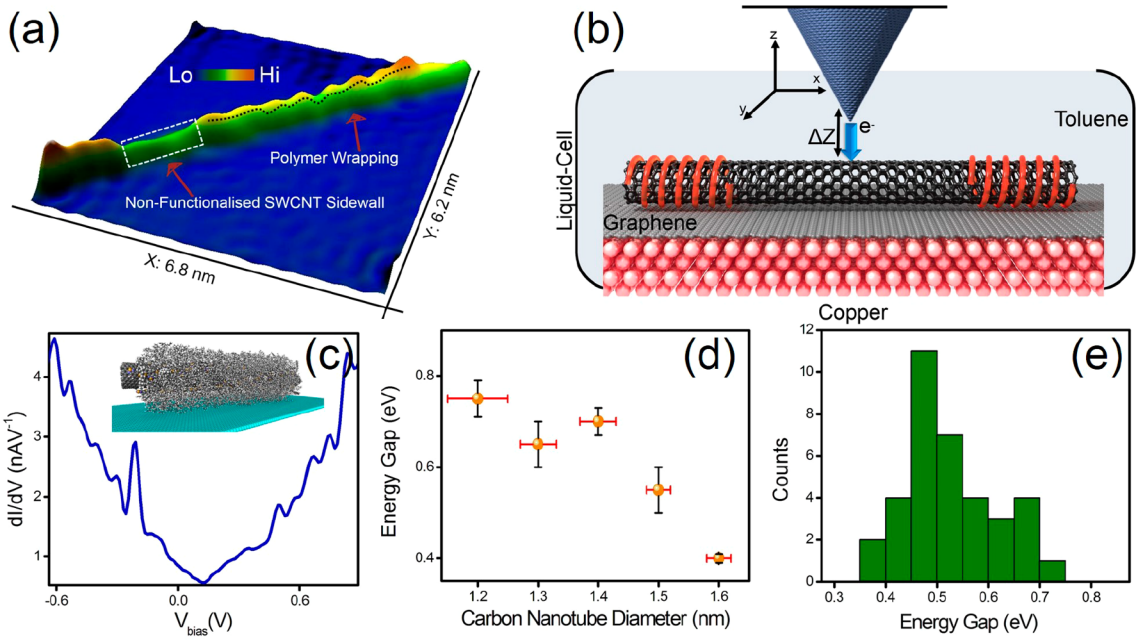

Figure 3. (a) Three-dimensionally represented constant-current STM image of a single PW-SWCNT in a toluene environment. The polymer wrapping along the carbon nanostructure is marked by black dashed lines. Areas where the polymer is missing are marked as a nonfunctionalized area within the white dashed rectangle. (Scan parameters: I_t = 4 pA, V_b = −0.8 V, scan rate = 18 Hz.) (b) Schematic for the local point probe spectroscopic analysis on the carbon nanostructure devoid of any polymeric wrapping over long intervals. (c) Differential conductance spectra acquired over the region indicated by the white rectangle in panel a. The difference in energy spacing between the sharp primary energetic peaks centered around −0.25 and +0.45 eV provide an energy gap of 0.65 eV (set point parameters: I_t = 180 pA, V_b = 0.5 V). The stark shift in the gaps to the right indicates hybridization of nanotube wave functions with the underlying Cu even in the presence of the graphene layer. The top inset in panel (c) is a snapshot of MD simulations of a PW-SWCNT on monatomic graphene lattice in the presence of a toluene molecules crowding around the hybrid complex. (d) Plot of core nanotube energy gap as a function of tube diameter measured on the nonfunctionalized region of individual nanotubes showing a trend where the tube diameter scales inversely with the measured energy gap. (e) Statistical analysis of the energy gap distribution measured on several PW-SWCNTs.

assembly on the nanotubes. Figure 3a is a high-resolution constant current large-area STM image of a PW-SWCNT complex where there is a much larger spacing between adjacent polymer strands (indicated by a white rectangle) when compared to the close packed polymer assembly with only smaller region where the core nanotube is nonfunctionalized as seen in the same figure (indicated by black dotted line) and in the inset STM image in Figure 2b. Performing local-point probe spectroscopy on the wide-spaced area devoid of any polymer wrapping over the region marked with white rectangle in Figure 3a and as schematically depicted in Figure 3b we observed marked difference in the spectral signature recorded over the bare nanotube region. A shift of the Fermi energy toward the valence band edge is observable from the differential conductance spectral curve (Figure 3c). Similar doped electronic structure was previously reported for semiconducting tubes deposited directly on Au(111) and the doping effect was attributed to charge transfer from the metallic *d*-bands into the energetic states of the nanotube.[32,38]

Conversely, in our experiments, the liquid-phase solubilized PW-SWCNTs were deposited onto graphene grown on Cu foil, wherein the single-layer graphene should serve as a spacer to electronically decouple the overlying carbon nanotube. However, it has been shown that the atomic lattice of graphene has topological imperfections such as point-defects[27,39] through which electrons could still tunnel through from the underlying Cu.[40] This result suggests that a tightly packed polymeric assembly on the carbon backbone tends to reduce the nanotube−metal electronic overlap. In cases where there is a large area of nonfunctionalized carbon backbone, as seen in Figure 3a, it can lead to metal induced hybridization of nanotube wave functions as seen from the shift in the energy gaps and the nonsymmetric positioning of the spectral curve around zero-bias voltage (Figure 3c).

Taken together, the spectroscopy data indicates two different spectral signatures; nanotube regions with closely assembled polymers (Figure 2b) that spatially distances the nanotube from the surface and comparatively larger areas of exposed nanotube regions with no polymer wrapping (Figure 3a), resulting in physical proximity with the underlying surface leading to hybridization of metal-nanotube energy levels (Figure 3c). In addition, the combined spectral analysis shows the measured energy gap to scale inversely with the diameter of the core nanotube (Figure 3d) emphasizing the role of diameter and local electrical contact of polymer assembly on the nanotube wave functions. The origin for the error bars in the plot of energy gap versus carbon nanotube diameter (Figure 3d) stems from the energetic shifts in the primary energetic peaks around the Fermi edge when measured on different carbon nanotubes at room-temperature as shown in the statistical distribution of the measured nanotube energy gaps (Figure 3e). The error bar in Figure 3d on each data point is a result of averaging over 15 different nanotubes located within the same sample. To check the reproducibility of the differential conductance spectra reported for the polymer wrapped nanotubes, each forward and reverse voltage sweep (tip stability and image resolution is constantly monitored) was analyzed for each individual case and reported only for reproducible spectral curves (forward and

DOI: 10.1021/acs.langmuir.8b00485
Langmuir 2018, 34, 6225−6230

reverse) obtained on the PW-SWCNTs which comply with the applied feedback loop settings.

CONCLUSIONS

In summary, the effect of polymer adsorption on the electronic structure of semiconducting carbon nanotubes adsorbed on graphene in solvent media has been registered through a combined scanning tunneling microscopy and spectroscopy investigation. The crystallinity of the polymeric strands remains conserved even after wrapping the nanotube sidewalls through multiple parallel modes. The differences in spectral signature for nanotubes as a function of the homogeneity and spacing of the polymer strands is resolved with high-energy resolution. The present data suggests that the polymer wrapping not only enriches the semiconducting nanotubes but also disentangles locally the nanotube backbone adsorbed on graphene from the bottom metallic contacts. Thus, the precise description of interfacial interactions of hybrid carbon nanomaterials even in chemically congested environments is a requisite for integration with emerging graphene devices.[41,42]

ASSOCIATED CONTENT

Supporting Information

The Supporting Information is available free of charge on the ACS Publications website at DOI: 10.1021/acs.langmuir.8b00485.

Preparation and characterization of PW-SWCNT dispersions, AFM, RAMAN and liquid-based probe microscopy details and molecular dynamics calculations (PDF)

AUTHOR INFORMATION

Corresponding Author

*E-mail: peter.nirmalraj@unifr.ch.

ORCID

Peter Nirmalraj: 0000-0002-2282-6781

Maria Antonietta Loi: 0000-0002-7985-7431

Present Address

⊥F.V.: Lincoln Laboratory, Massachusetts Institute of Technology, MA 02421-6426, United States.

Notes

The authors declare no competing financial interest.

ACKNOWLEDGMENTS

M.C.S. gratefully acknowledges M. Terrones for granting access to the Materials Studio package at Penn State University and to Fundação de Amparo à Pesquisa do Estado de São Paulo for financial support. P.N. thanks Miguel Spuch-Calvar for assistance with schematics. M.A.L. and U.S. acknowledge Stichting voor Technische Wetenschappen (STW, Utrecht, The Netherlands) and the Deutsche Forschungsgemeinschaft (DFG, Bonn, Germany) for the funding of the collaborative research between the University of Groningen and Wuppertal University. The Groningen group is thankful to A. Kamp and T. Zaharia for technical support. This work is part of the research programme FOM-focus Group "Next Generation Organic Photovoltaics" participating in the Dutch Institute for Fundamental Energy Research (DIFFER).

REFERENCES

(1) Park, H.; Afzali, A.; Han, S.-J.; Tulevski, G. S.; Franklin, A. D.; Tersoff, J.; Hannon, J. B.; Haensch, W. High-density integration of carbon nanotubes via chemical self-assembly. *Nat. Nanotechnol.* **2012**, *7* (12), 787−791.

(2) Bachtold, A.; Hadley, P.; Nakanishi, T.; Dekker, C. Logic Circuits with Carbon Nanotube Transistors. *Science* **2001**, *294* (5545), 1317−1320.

(3) Cao, Q.; Tersoff, J.; Farmer, D. B.; Zhu, Y.; Han, S.-J. Carbon nanotube transistors scaled to a 40-nanometer footprint. *Science* **2017**, *356* (6345), 1369−1372.

(4) Samanta, S. K.; Fritsch, M.; Scherf, U.; Gomulya, W.; Bisri, S. Z.; Loi, M. A. Conjugated Polymer-Assisted Dispersion of Single-Wall Carbon Nanotubes: The Power of Polymer Wrapping. *Acc. Chem. Res.* **2014**, *47* (8), 2446−2456.

(5) Salazar-Rios, J. M.; Gomulya, W.; Derenskyi, V.; Yang, J.; Bisri, S. Z.; Chen, Z.; Facchetti, A.; Loi, M. A. Selecting Semiconducting Single-Walled Carbon Nanotubes with Narrow Bandgap Naphthalene Diimide-Based Polymers. *Advanced Electronic Materials* **2015**, *1* (8), 1500074.

(6) Deria, P.; Von Bargen, C. D.; Olivier, J.-H.; Kumbhar, A. S.; Saven, J. G.; Therien, M. J. Single-Handed Helical Wrapping of Single-Walled Carbon Nanotubes by Chiral, Ionic, Semiconducting Polymers. *J. Am. Chem. Soc.* **2013**, *135* (43), 16220−16234.

(7) Kourkouli, S. N.; Siokou, A.; Stefopoulos, A. A.; Ravani, F.; Plocke, T.; Müller, M.; Maultzsch, J.; Thomsen, C.; Papagelis, K.; Kallitsis, J. K. Electronic Properties of Semiconducting Polymer-Functionalized Single Wall Carbon Nanotubes. *Macromolecules* **2013**, *46* (7), 2590−2598.

(8) Gao, J.; Loi, M. A.; de Carvalho, E. J. F.; dos Santos, M. C. Selective Wrapping and Supramolecular Structures of Polyfluorene−Carbon Nanotube Hybrids. *ACS Nano* **2011**, *5* (5), 3993−3999.

(9) Wang, H.; Bao, Z. Conjugated polymer sorting of semiconducting carbon nanotubes and their electronic applications. *Nano Today* **2015**, *10* (6), 737−758.

(10) Derenskyi, V.; Gomulya, W.; Talsma, W.; Salazar-Rios, J. M.; Fritsch, M.; Nirmalraj, P.; Riel, H.; Allard, S.; Scherf, U.; Loi, M. A. On-Chip Chemical Self-Assembly of Semiconducting Single-Walled Carbon Nanotubes (SWNTs): Toward Robust and Scale Invariant SWNTs Transistors. *Adv. Mater.* **2017**, *29*, 1606757.

(11) Lee, H. W.; Yoon, Y.; Park, S.; Oh, J. H.; Hong, S.; Liyanage, L. S.; Wang, H.; Morishita, S.; Patil, N.; Park, Y. J.; Park, J. J.; Spakowitz, A.; Galli, G.; Gygi, F.; Wong, P. H. S.; Tok, J. B. H.; Kim, J. M.; Bao, Z. Selective dispersion of high purity semiconducting single-walled carbon nanotubes with regioregular poly(3-alkylthiophene)s. *Nat. Commun.* **2011**, *2*, 541.

(12) Wong, M. H.; Giraldo, J. P.; Kwak, S.-Y.; Koman, V. B.; Sinclair, R.; Lew, T. T. S.; Bisker, G.; Liu, P.; Strano, M. S. Nitroaromatic detection and infrared communication from wild-type plants using plant nanobionics. *Nat. Mater.* **2017**, *16* (2), 264−272.

(13) Giraldo, J. P.; Landry, M. P.; Faltermeier, S. M.; McNicholas, T. P.; Iverson, N. M.; Boghossian, A. A.; Reuel, N. F.; Hilmer, A. J.; Sen, F.; Brew, J. A.; Strano, M. S. Plant nanobionics approach to augment photosynthesis and biochemical sensing. *Nat. Mater.* **2014**, *13* (4), 400−408.

(14) Kim, S.; Yoon, J.; Kim, H.-D.; Choi, S.-J. Carbon Nanotube Synaptic Transistor Network for Pattern Recognition. *ACS Appl. Mater. Interfaces* **2015**, *7* (45), 25479−25486.

(15) Zhao, W. S.; Agnus, G.; Derycke, V.; Filoramo, A.; Bourgoin, J. P.; Gamrat, C. Nanotube devices based crossbar architecture: toward neuromorphic computing. *Nanotechnology* **2010**, *21* (17), 175202.

(16) Bonhommeau, S.; Deria, P.; Glesner, M. G.; Talaga, D.; Najjar, S.; Belin, C.; Auneau, L.; Trainini, S.; Therien, M. J.; Rodriguez, V. Raman Spectroscopic Investigation of Individual Single-Walled Carbon Nanotubes Helically Wrapped by Ionic, Semiconducting Polymers. *J. Phys. Chem. C* **2013**, *117* (28), 14840−14849.

(17) Star, A.; Stoddart, J. F.; Steuerman, D.; Diehl, M.; Boukai, A.; Wong, E. W.; Yang, X.; Chung, S.-W.; Choi, H.; Heath, J. R.

DOI: 10.1021/acs.langmuir.8b00485
Langmuir 2018, 34, 6225−6230

Preparation and Properties of Polymer-Wrapped Single-Walled Carbon Nanotubes. *Angew. Chem., Int. Ed.* **2001**, *40* (9), 1721−1725.
(18) Waclawik, E. R.; Bell, J. M.; Goh, R. G. S.; Musumeci, A.; Motta, N. Self-organization in composites of poly(3-hexylthiophene) and single-walled carbon nanotubes designed for use in photovoltaic applications. *Proc. SPIE 6036, BioMEMS and Nanotechnology II* **2006**, 603607.
(19) Giulianini, M.; Waclawik, E. R.; Bell, J. M.; Scarselli, M.; Castrucci, P.; De Crescenzi, M.; Motta, N. Microscopic and Spectroscopic Investigation of Poly(3-hexylthiophene) Interaction with Carbon Nanotubes. *Polymers* **2011**, *3* (3), 1433.
(20) Geng, J.; Kong, B.-S.; Yang, S. B.; Youn, S. C.; Park, S.; Joo, T.; Jung, H.-T. Effect of SWNT Defects on the Electron Transfer Properties in P3HT/SWNT Hybrid Materials. *Adv. Funct. Mater.* **2008**, *18* (18), 2659−2665.
(21) Shim, M.; Ozel, T.; Gaur, A.; Wang, C. Insights on Charge Transfer Doping and Intrinsic Phonon Line Shape of Carbon Nanotubes by Simple Polymer Adsorption. *J. Am. Chem. Soc.* **2006**, *128* (23), 7522−7530.
(22) Cao, Q.; Han, S.-j.; Tulevski, G. S.; Zhu, Y.; Lu, D. D.; Haensch, W. Arrays of single-walled carbon nanotubes with full surface coverage for high-performance electronics. *Nat. Nanotechnol.* **2013**, *8* (3), 180−186.
(23) Strano, M. S.; Dyke, C. A.; Usrey, M. L.; Barone, P. W.; Allen, M. J.; Shan, H.; Kittrell, C.; Hauge, R. H.; Tour, J. M.; Smalley, R. E. Electronic Structure Control of Single-Walled Carbon Nanotube Functionalization. *Science* **2003**, *301* (5639), 1519−1522.
(24) Wang, X.; Azimi, H.; Mack, H.-G.; Morana, M.; Egelhaaf, H.-J.; Meixner, A. J.; Zhang, D. Probing the Nanoscale Phase Separation and Photophysics Properties of Low-Bandgap Polymer:Fullerene Blend Film by Near-Field Spectroscopic Mapping. *Small* **2011**, *7* (19), 2793−2800.
(25) Nirmalraj, P. N.; Thompson, D.; Riel, H. E. Capturing the embryonic stages of self-assembly - design rules for molecular computation. *Sci. Rep.* **2015**, *5*, 10116.
(26) Nirmalraj, P.; La Rosa, A.; Thompson, D.; Sousa, M.; Martin, N.; Gotsmann, B.; Riel, H. Fingerprinting Electronic Molecular Complexes in Liquid. *Sci. Rep.* **2016**, *6*, 19009.
(27) Nirmalraj, P.; Thompson, D.; Dimitrakopoulos, C.; Gotsmann, B.; Dumcenco, D.; Kis, A.; Riel, H. A robust molecular probe for Ångstrom-scale analytics in liquids. *Nat. Commun.* **2016**, *7*, 12403.
(28) Nirmalraj, P.; Daly, R.; Martin, N.; Thompson, D. Motion of Fullerenes around Topological Defects on Metals: Implications for the Progress of Molecular Scale Devices. *ACS Appl. Mater. Interfaces* **2017**, *9* (9), 7897−7902.
(29) Czerw, R.; Guo, Z.; Ajayan, P. M.; Sun, Y.-P.; Carroll, D. L. Organization of Polymers onto Carbon Nanotubes: A Route to Nanoscale Assembly. *Nano Lett.* **2001**, *1* (8), 423−427.
(30) O'Connell, M. J.; Boul, P.; Ericson, L. M.; Huffman, C.; Wang, Y.; Haroz, E.; Kuper, C.; Tour, J.; Ausman, K. D.; Smalley, R. E. Reversible water-solubilization of single-walled carbon nanotubes by polymer wrapping. *Chem. Phys. Lett.* **2001**, *342* (3−4), 265−271.
(31) Odom, T. W.; Huang, J.-L.; Kim, P.; Lieber, C. M. Atomic structure and electronic properties of single-walled carbon nanotubes. *Nature* **1998**, *391* (6662), 62−64.
(32) Wilder, J. W. G.; Venema, L. C.; Rinzler, A. G.; Smalley, R. E.; Dekker, C. Electronic structure of atomically resolved carbon nanotubes. *Nature* **1998**, *391* (6662), 59−62.
(33) Lin, H.; Lagoute, J.; Repain, V.; Chacon, C.; Girard, Y.; Lauret, J. S.; Ducastelle, F.; Loiseau, A.; Rousset, S. Many-body effects in electronic bandgaps of carbon nanotubes measured by scanning tunnelling spectroscopy. *Nat. Mater.* **2010**, *9* (3), 235−238.
(34) Peet, J.; Kim, J. Y.; Coates, N. E.; Ma, W. L.; Moses, D.; Heeger, A. J.; Bazan, G. C. Efficiency enhancement in low-bandgap polymer solar cells by processing with alkane dithiols. *Nat. Mater.* **2007**, *6* (7), 497−500.
(35) Ghasempour, H.; Azhdari Tehrani, A.; Morsali, A.; Wang, J.; Junk, P. C. Two pillared metal-organic frameworks comprising a long pillar ligand used as fluorescent sensors for nitrobenzene and heterogeneous catalysts for the Knoevenagel condensation reaction. *CrystEngComm* **2016**, *18* (14), 2463−2468.
(36) Milko, M.; Puschnig, P.; Blondeau, P.; Menna, E.; Gao, J.; Loi, M. A.; Draxl, C. Evidence of Hybrid Excitons in Weakly Interacting Nanopeapods. *J. Phys. Chem. Lett.* **2013**, *4* (16), 2664−2667.
(37) Kahmann, S.; Salazar Rios, J. M.; Zink, M.; Allard, S.; Scherf, U.; dos Santos, M. C.; Brabec, C. J.; Loi, M. A. Excited-State Interaction of Semiconducting Single-Walled Carbon Nanotubes with Their Wrapping Polymers. *J. Phys. Chem. Lett.* **2017**, *8* (22), 5666−5672.
(38) Pham, V. D.; Repain, V.; Chacon, C.; Bellec, A.; Girard, Y.; Rousset, S.; Campidelli, S.; Lauret, J.-S.; Voisin, C.; Terrones, M.; dos Santos, M. C.; Lagoute, J. Properties of Functionalized Carbon Nanotubes and Their Interaction with a Metallic Substrate Investigated by Scanning Tunneling Microscopy. *J. Phys. Chem. C* **2017**, *121* (43), 24264−24271.
(39) Banhart, F.; Kotakoski, J.; Krasheninnikov, A. V. Structural Defects in Graphene. *ACS Nano* **2011**, *5* (1), 26−41.
(40) Nirmalraj, P. N.; Thodkar, K.; Guerin, S.; Calame, M.; Thompson, D. Graphene wrinkle effects on molecular resonance states. *npj 2D Mater. Appl.* **2018**, *2* (1), 8.
(41) Pósa, L.; El Abbassi, M.; Makk, P.; Sánta, B.; Nef, C.; Csontos, M.; Calame, M.; Halbritter, A. Multiple Physical Time Scales and Dead Time Rule in Few-Nanometers Sized Graphene−SiOx-Graphene Memristors. *Nano Lett.* **2017**, *17* (11), 6783−6789.
(42) Li, Y.; Yu, H.; Qiu, X.; Dai, T.; Jiang, J.; Wang, G.; Zhang, Q.; Qin, Y.; Yang, J.; Jiang, X. Graphene-based nonvolatile terahertz switch with asymmetric electrodes. *Sci. Rep.* **2018**, *8* (1), 1562.

DOI: 10.1021/acs.langmuir.8b00485
Langmuir 2018, 34, 6225−6230